

ORIGINAL ARTICLE

Complex Congenital Heart Disease Associated With Disordered Myocardial Architecture in a Midtrimester Human Fetus

See Editorial by Sosnovik and Geva

BACKGROUND: In the era of increasingly successful corrective interventions in patients with congenital heart disease (CHD), global and regional myocardial remodeling are emerging as important sources of long-term morbidity/mortality. Changes in organization of the myocardium in CHD, and in its mechanical properties, conduction, and blood supply, result in altered myocardial function both before and after surgery. To gain a better understanding and develop appropriate and individualized treatment strategies, the microscopic organization of cardiomyocytes, and their integration at a macroscopic level, needs to be completely understood. The aim of this study is to describe, for the first time, in 3 dimensions and nondestructively the detailed remodeling of cardiac microstructure present in a human fetal heart with complex CHD.

METHODS AND RESULTS: Synchrotron X-ray phase-contrast imaging was used to image an archival midgestation formalin-fixed fetal heart with right isomerism and complex CHD and compare with a control fetal heart. Analysis of myocyte aggregates, at detail not accessible with other techniques, was performed. Macroanatomic and conduction system changes specific to the disease were clearly observable, together with disordered myocyte organization in the morphologically right ventricle myocardium. Electrical activation simulations suggested altered synchronicity of the morphologically right ventricle.

CONCLUSIONS: We have shown the potential of X-ray phase-contrast imaging for studying cardiac microstructure in the developing human fetal heart at high resolution providing novel insight while preserving valuable archival material for future study. This is the first study to show myocardial alterations occur in complex CHD as early as midgestation.

Patricia Garcia-Canadilla, PhD
Hector Dejea, MSc
Anne Bonnin, PhD
Vedrana Balicevic, MSc
Sven Loncaric, PhD
Chong Zhang, PhD
Constantine Butakoff, PhD
Jazmin Aguado-Sierra, PhD
Mariano Vázquez, PhD
Laurence H. Jackson, PhD
Daniel J. Stuckey, PhD
Cristoph Rau, PhD
Marco Stampanoni, PhD
Bart Bijmens, PhD*
Andrew C. Cook, PhD*

*Drs Bijmens and Cook contributed equally to this work.

Key Words: fetal heart ■ humans
■ isomerism ■ myocardium
■ synchrotrons ■ X-ray microtomography

© 2018 American Heart Association, Inc.

<https://www.ahajournals.org/journal/circimaging>

CLINICAL PERSPECTIVE

This is a first, proof-of-principle study, which demonstrates myocardial disorganization in a human fetus with complex congenital heart disease in the midgestation of pregnancy using the novel technique of synchrotron X-ray phase-contrast imaging. It shows it is possible to image in 3-dimensional and nondestructively, the detailed cardiac microstructure present in an ex vivo human fetal heart, opening up new areas of research into structure/function of the fetal myocardium. Macroanatomic changes and conduction system changes specific to the disease are described, together with disordered myocyte organization in basal, septal, and morphologically right ventricular myocardium. These findings are clinically relevant because in this particular fetus, the morphologically left ventricle was small and the parents had been counseled of the likelihood of a functionally univentricular palliation being required after birth with the morphologically right ventricle becoming the systemic ventricle. We cannot predict how the morphological right ventricle would have developed through subsequent gestation, and postnatally, and it is possible that there would have been delayed recovery with normal remodeling of the right ventricular myocardium later in gestation. It is also possible that the regional wall disorganization documented in this heart could have persisted and led to abnormal regional function and wall stresses, contributing to abnormal global function and development of remodeling and fibrosis later in pregnancy and postnatally. Further work using this new technique to examine a spectrum of fetal structural heart disease is warranted.

Congenital heart disease (CHD) is the leading cause of infant morbidity in developed countries and affects $\approx 1\%$ of newborns.¹ For most phenotypes of CHD, effective corrective or palliative interventions have been developed. Although an adequate circulation can mostly be established, long-term morbidity and mortality is still an important clinical problem, especially those related to heart (myocardial) failure and remodeling. Therefore, besides basic morphology, detailed knowledge of the microarchitecture of the heart and its complex (altered) development is essential, not only for understanding the genesis of CHD and addressing long-term consequences of the disease but also for developing realistic biophysical computational models as a precursor to new or personalized treatment strategies.

Myocytes are aggregated and aligned in a predominant direction within the atrial and ventricular

walls, forming a complex 3-dimensional (3D) network (myocardial architecture). The complex organization of these bundles of myocytes within the myocardium determines the propagation of electrical waves as well as the force development within cardiac tissue. Understanding altered contractile function and triggers for remodeling requires knowledge of this organization. Data on the organization of the myocardium in fetal life useful for computational modeling is limited, and even our understanding of normal myocardial architecture after birth and in adulthood is still under debate.^{2,3} Even less is known about the microstructure of structurally abnormal hearts, especially given the complexity of CHD and the great variety of underlying phenotypes.⁴

Therefore, comparing the organization of the myocardium in different forms of CHD, and quantifying the overall and detailed differences in comparison with normal hearts, is essential for a better understanding of normal and abnormal cardiac architecture, to target long-term corrective therapy and to parametrize computational modeling of myocardial development, electrical propagation, and resulting function.

To identify and quantify cardiac microstructure and to image the whole heart for evaluating detailed shape and macrostructure, high-resolution imaging (in the order of only a few microns) is required. A number of 3D imaging techniques can be used for assessing detailed cardiac morphology at high resolutions. However, only few of them allow imaging a whole heart volume in 3D nondestructively. Optical (episcopic) microscopy is able to acquire the information needed at high enough contrast and resolution but is limited to in vitro imaging and additionally requires the destruction of the sample.⁵ High-resolution magnetic resonance imaging (MRI) can provide reasonable resolution and contrast for myocardial macrostructure but to image microstructure requires the addition of directional sampling in diffusion tensor MRI (DT-MRI), necessitates extremely long scan times, and is still relatively limited in resolution, especially in vivo.⁶ Classical, absorption-based micro-CT shows promise, is fast, has resolution to identify individual cardiomyocytes (in adults) but requires iodine staining to provide adequate contrast.^{7,8} Novel high-resolution imaging techniques, such as synchrotron X-ray phase-contrast imaging (X-PCI), have already demonstrated good results in the study of structural changes of hearts from rabbit fetuses, young rats, and human fetuses at micrometer resolution,^{9–12} with sufficient contrast to distinguish myocytes at cellular level and without the need for destructive sectioning, tissue processing, or the use of contrast agents.

This study focuses on the detailed analysis of a human fetal heart with complex CHD and a control, as a proof of principle. Specifically, the abnormal heart we

analyzed was from a fetus with a defect of laterality, termed isomerism, involving multiorgan abnormalities and complex CHD. We provide for the first time details, currently not accessible with other imaging techniques, of the microstructure of this heart by means of X-PCI, which suggest myocardial abnormalities are indeed present in CHD before birth from the midtrimester of pregnancy. We also show that the accurate measurement of the complex 3D arrangement of myocytes within the myocardium, together with detailed cardiac geometry, allows detailed computational cardiac electrical activation simulations, providing new insights into functional and electromechanical remodeling in CHD.

METHODS

The data will be made available to other researchers for purposes of reproducing the results.¹³

Sample Description

The samples used in this study are from the Cardiac Archive, held at the Institute of Child Health, under UK Human Tissue Authority Research Licence (No. 12220). The study, including transportation of samples, was approved by the Institute's Human Tissue Authority research committee and the research committee of the Cardiac Academic Group, Children's Cardiovascular Research Department (Great Ormond Street Hospital/Institute of Cardiovascular Science). First, a heart of 20 weeks of gestation with complex CHD was selected. The selected heart showed right isomerism (bilateral right atrial appendages); a right-sided heart and apex; mirror image arrangement of the ventricles (left-handed ventricular topology or I loop); atrioventricular septal defect with common atrioventricular junction and valve; and pulmonary atresia with aorta from the morphologically right ventricle (mRV). In the donating fetus, both lungs were trilobed, bronchi short and eparterial, stomach left sided, gallbladder right sided, liver central, spleen absent, and intestines normally rotated. Prenatal diagnosis at 20 weeks' gestation had shown normal fetal head, brain, face, spine, neck, skin, chest, abdominal wall, gastrointestinal tract, kidneys and bladder, extremities, and skeleton. Image quality was limited, but complex CHD was identified comprising right isomerism, right-sided heart and apex, biventricular atrioventricular connection, left-hand ventricular topology, unbalanced atrioventricular septal defect with common atrioventricular valve and right ventricular dominance, single outlet with aorta from mRV, and pulmonary atresia. Abnormal pulmonary venous Doppler suggested obstruction to pulmonary veins, but drainage of pulmonary veins was not clearly identified. There was retrograde flow in the arterial duct and small central pulmonary arteries. The heart was noted to be in sinus rhythm. This amounted to complex CHD with functionally single ventricle and palliative surgery as the likely course postnatally. The parents opted for termination of pregnancy and consented for autopsy and retention of the fetal heart for research purposes.

For comparison, a normal fetal heart of 19 weeks of gestation was chosen from the same historical collection. Notes show termination of pregnancy for social reasons, and the fetus had no cardiac or extracardiac abnormalities.

Data Acquisition

X-Ray Phase-Contrast Imaging

Imaging of the heart with complex CHD heart was performed at the TOMCAT beamline of the Swiss Light Source (PSI, Switzerland), with X-ray propagation-based phase-contrast tomography, using a 20-keV parallel synchrotron X-ray beam (monochromaticity bandwidth of 2%). The sample was located 60 cm from the detector (camera: sCMOS pco.EDGE 5.5; scintillator: LAG:Ce 300 μm). The field of view was 13.03×3.2 mm² with isotropic pixel size of 5.2 μm . The sample was kept at room temperature placed in a sealed plastic tube with degassed deionized water and secured on a sample holder.

After positioning the heart at the stage's center of rotation, acquisition was performed by rotating the sample through 360° acquiring 2500 projections (exposure time, 70 ms). Nine sequential acquisitions (overlap, 126 slices, 0.66 mm) from base to apex were performed to cover the whole heart along its longitudinal axis. Additionally, 50 flat and 20 dark images were acquired for flat-field and dark-field corrections of each acquisition. Before the reconstruction procedure, a single-distance phase-retrieval approach, the Paganin filter,¹⁴ was applied on each projection to improve visualization of the cardiac tissue. The projection set was finally reconstructed, both with and without Paganin filter, using the Gridrec algorithm.¹⁵ Reconstructed volumes were then merged together to obtain a unique single data set for the whole heart with a Matlab script.

The normal heart was scanned at the I13-2 beamline of Diamond Light Source under similar conditions. Briefly, image acquisition was made using a 20-keV parallel synchrotron X-ray beam. The sample was located 120 cm from the detector (camera: pco.4000 with a 1.25× objective lens; scintillator: CAWO4 250 μm). The field of view was 14×9.6 mm with isotropic pixel size of 3.2 μm . Two thousand one projections of 0.5 second exposure time were recorded. Additionally, 20 flat and 20 dark images were acquired for flat-field and dark-field corrections, applied before the reconstruction procedure. The projection set was reconstructed using the filtered back-projection algorithm.

MRI Diffusion Tensor Image

MRI measurements were performed using a 9.4T horizontal bore scanner (Agilent Technologies, Santa Clara) equipped with 1000 mT/m gradient inserts and a 26-mm volume resonator RF coil (RAPID Biomedical, Rimpf, Germany). 3D fast spin echo DT-MRI acquisition with monopolar diffusion weighting gradients was performed in the heart with complex CHD (maximum gradient strength, 26 G/cm). Acquisition parameters were isotropic resolution, 156 μm ; field of view, 2 cm³; repetition time/echo time, 600/18 ms; flip angle, 90°; with 3 spatial averages. Diffusion weighting was applied in 30 directions with 3 unweighted b₀ volumes, with diffusion weighting of b=1180 s/mm², gradient strength of 0.26 T/m, duration of 0.5 ms, and separation of 10 ms.

Image Analysis

Tissue and Arterial Tree Segmentation

Datasets were analyzed with Fiji (reslicing/rendering), and image analysis software Ilastik¹⁶ (image segmentation). Segmentation of Paganin reconstructed dataset was performed semiautomatically using the 2-stage pixel

classification module in Ilastik. Then, morphological operations were applied to smooth segmentations using first an in-house algorithm implemented in Matlab (R2016b; The MathWorks, Inc, Natick, MA, 2016) and second the Seg3D image processing software.¹⁷ Coronary arteries were manually segmented by labeling some slices and then performing a 3D interpolation in 3DSlicer.¹⁸

Delineation of the Conduction Tissue

Conduction tissue was visualized as low-density (dark) regions surrounded by connective tissue visible as high-density (bright) areas within the X-PCI images as described in previous studies of normal fetal and postnatal human hearts.^{11,19} The obtained dataset was rotated and resliced in Fiji to investigate the cardiac conduction system. To improve the visualization of conduction tissue, maximum-intensity projection (depth, 5 slices) was performed in the resliced dataset, to improve contrast between differing cardiac tissues. The components of the conduction system, including the atrioventricular node, nonbranching, left and right bundle branches, were manually traced in Seg3D software.¹⁷ 3D interpolation of delineated areas was performed to obtain a 3D volume reconstruction of the whole conduction system in 3DSlicer.¹⁸

Quantification of the Myocyte Aggregates Orientation

X-Ray Phase-Contrast Imaging

The gradient structure tensor was calculated on the reconstructed image dataset without Paganin filter to estimate the local orientation of the myocyte aggregates as described in the studies by Gonzalez-Tendero et al¹⁰ and Baličević et al.¹² Briefly, the oriented gradient magnitude in x, y and z directions was obtained for each voxel using a central difference algorithm. Then, the local structure tensor within a voxel's cubical neighborhood was calculated. Eigen decomposition of the structure tensor was performed to transform the given gradient space into a space with 3 orthogonal vectors. The smallest eigenvalue (λ_3), which indicated the direction with the lowest intensity variation, corresponds to the vector pointing in the myocyte direction, v_3 . For the smallest eigenvalues' vector v_3 , the helical angle (HA) α_H was calculated as the angle between the transverse plane and the vector projection to the local tangential plane of the cylindrical coordinate system of the heart (Figure 1A and 1B in the [Data Supplement](#)).

Detail of the quantification of the HA distribution within both ventricles is provided in Methods in the [Data Supplement](#).

MRI Diffusion Tensor Image

Intensity-based thresholding plus manual labeling was performed on baseline images to obtain a mask of the cardiac tissue. The segmented mask was applied to all the diffusion weighting images. DT-MRI was estimated in the masked volume using Camino²⁰ with a nonlinear optimization method. Eigenvalues and eigenvectors of the diffusion tensor were computed, and the principal eigenvector v_1 , describing the main myocyte aggregates direction, was considered to obtain the HA, computed as described in the previous section.

Computational Modeling of Electrical Activation

Details about the simulations of the electrical activation propagation are provided in Methods in the [Data Supplement](#).

RESULTS

Visualization of the Overall Cardiac Structure and Vasculature

Figure 1 displays example images obtained from the heart with complex CHD, reconstructed using the Gridrec algorithm¹⁵ and the Paganin phase-retrieval method¹⁴ showing short-axis slices at midventricular (Figure 1A) and atrioventricular valve level (Figure 1B), as well as a longitudinal resliced image through the common atrioventricular valve and apex (Figure 1C). The structure of the 3 segments of the heart (atria, ventricles, and great arteries) can be clearly differentiated and analyzed together with substructures, such as atrioventricular and arterial valvar complexes, including fine detail of tendinous cords and valvar leaflets (Figure 1D and 1E).

When visualizing data using volume rendering (Figure 2; Movie I in the [Data Supplement](#)) the complete structure of the cardiac segments can be identified. Compatible with right isomerism, there are bilaterally extensive pectinate muscles, as seen in short axis (Figure 2C). The ventriculoarterial connection is also evident, with a patent aortic valve arising from the left-sided mRV and pulmonary atresia. Hypoplastic sinuses are seen within the atretic pulmonary root, which would not be visible by standard techniques of dissection. The type and mode of atrioventricular connection is also clearly seen. There is a biventricular atrioventricular connection via a common atrioventricular junction, guarded by a common atrioventricular valve in the setting of an atrioventricular septal defect.

Location of the Conduction System in the Abnormal Fetal Heart

Figure 3 shows the feasibility of manual delineation of the conduction tissue in X-PCI images. Using similar methodology to that used in serial histological sections,^{21,22} the conduction system was traced section to section through the heart. Dual atrioventricular nodes were identified, 1 superiorly and 1 inferiorly joined by a sling of conduction tissue (common bundle). The connection from the superior atrioventricular node to the common bundle was narrower than the connection inferiorly. The ventricular bundle branches were readily identified arising from the common bundle astride the mid portion of the ventricular septum. Our findings agree with those

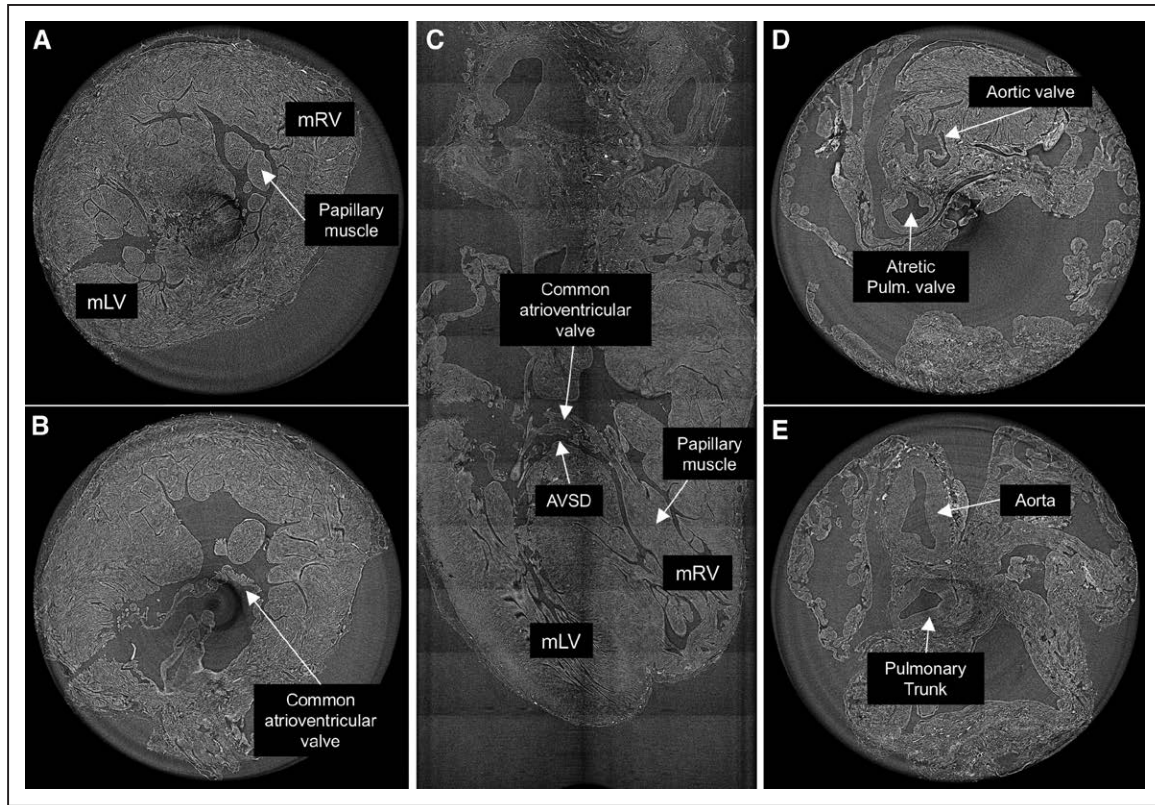


Figure 1. X-ray phase-contrast synchrotron radiation-based micro-computed tomographic imaging of complex congenital heart disease.

Short-axis (A and B) and longitudinal resliced images (C) showing detail of papillary muscles (A), common atrioventricular valve (B and C), aortic and tricuspid valves (D), the aorta, and pulmonary trunk (E). AVSD indicates atrioventricular septal defect; mLV, morphologically left ventricle; and mRV, morphologically right ventricle.

reported in similar fetal specimens with right isomerism and left-hand topology.^{21,22} A 3D reconstruction of the manually delineated conduction system,

including both atrioventricular nodes, common, left, and right bundle branches, is shown in Figure 3B and 3C and in Movie II in the [Data Supplement](#).

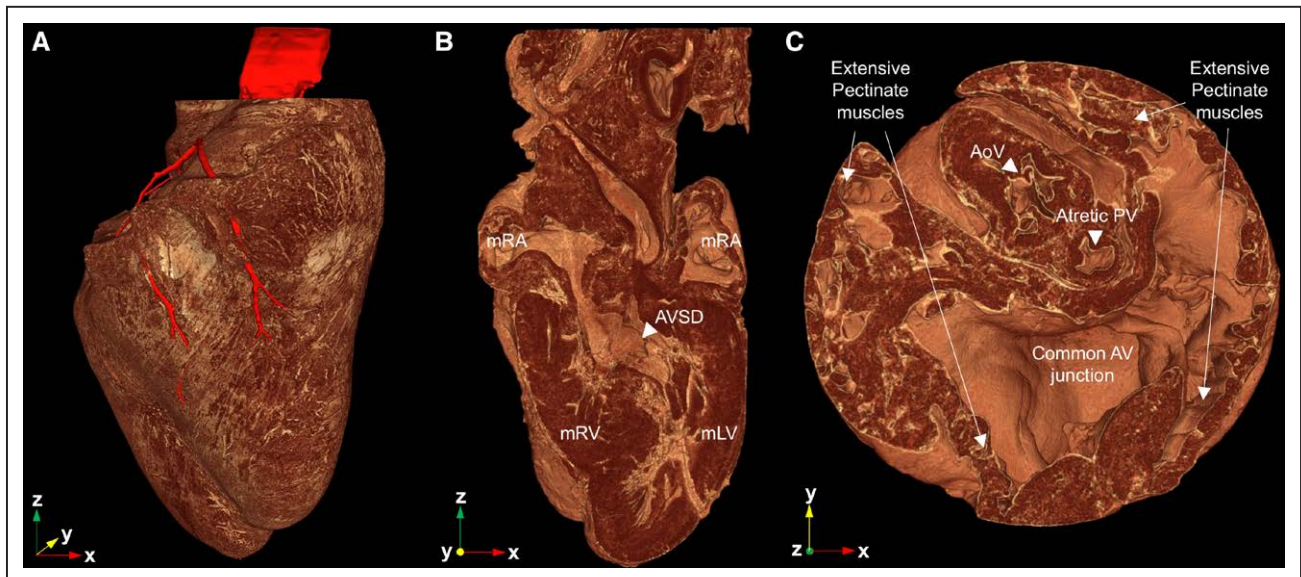


Figure 2. Detailed visualization of cardiac anatomy and vasculature.

A, Volume rendered image depicting detailed cardiac anatomy together with proximal coronary tree (red). B, Longitudinal and (C) short-axis virtual cuts of the 3-dimensional volume render showing details of abnormal anatomy, including atrioventricular septal defect (AVSD), extensive pectinate muscles, and atretic pulmonary valve. AoV indicates aortic valve; AV, atrioventricular; mLA, morphologically left atrium; mLV, morphologically left ventricle; mRA, morphologically right atrium; mRV, morphologically right ventricle; and PV, pulmonary valve.

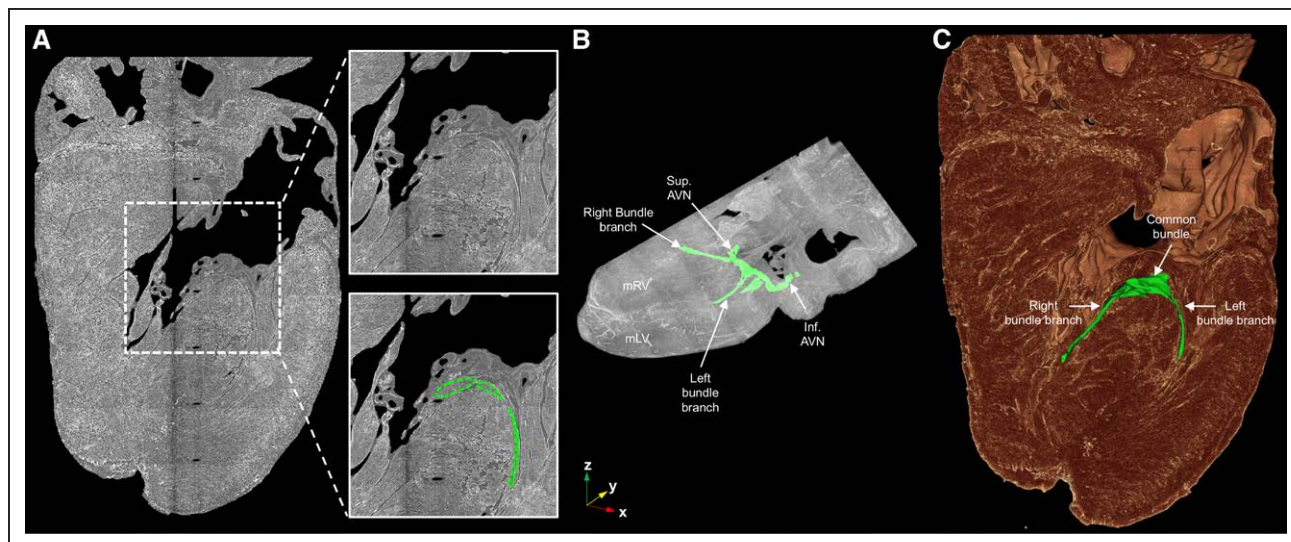


Figure 3. Delineation and 3-dimensional (3D) reconstruction of the conduction system in complex congenital heart disease. **A**, Virtual longitudinal cut of the resliced X-ray phase-contrast imaging (X-PCI) dataset showing delineation of the conduction tissue (dashed green line). **B**, Maximum-intensity projection of the X-PCI dataset together with 3D rendering showing 2 atrioventricular nodes (AVNs) connected by a sling of conduction tissue (green). **C**, Volumetric reconstruction and 3D representation of the conduction system (green) showing the common, left, and right bundle branches. Inf. indicates inferior; mLV, morphologically left ventricle; mRV, morphologically right ventricle; and Sup., superior.

Myocyte Aggregate Orientation

A longitudinal plane of the calculated HA of myocyte aggregates together with the visualization of the resulting 3D vector plots within 4 different apical-basal short-axis slices of the normal and complex CHD fetal hearts, together with an overall rendering of the resulting 3D fiber structure, is shown in Figure 4. The myoarchitecture of the morphologically left ventricle (mLV) in the abnormal and control hearts shows a gradual change in HA from epicardium to endocardium as has been showed in adults.²³ However, in the heart with complex CHD, the middle layer of circumferential myocytes is thicker and the deep layer of longitudinal cardiomyocytes thinner compared with the control. Regional areas of more disorganized myocytes are evident in the septal and free wall of the mRV as reflected in the plots of HA within select slices (Figure 4). Moreover, a flipping of the myocardial pattern within the mid septal wall is evident; myocyte orientation in the apex is normal but changes to a partially mirror-imaged transmural distribution at the base, similar to that seen in *situs inversus totalis*.²⁴

Figure 5 shows the comparison of local HAs determined by X-PCI (Figure 5A) and DT-MRI (Figure 5B) within 2 slices (apical and mid ventricular). Although the overall pattern is qualitatively similar, both show the clear disorganization of myocyte aggregates within the septum and mRV in midventricular slices; the low resolution of DT-MRI images (demonstrated by limited voxels across the lateral wall) makes it more difficult to see the gradual change in the local HA from endocardium to epicardium clearly present in the X-PCI images.

Disorganization in the septum of the isomeric heart is also evident when quantitatively comparing the transmural

profiles of HA with the normal control heart (Figure 6), showing a lower linear correlation ($R^2=0.81\pm 0.19$ normal versus 0.63 ± 0.26 CHD; Table I in the [Data Supplement](#)).

Finally, according to the distribution of HAs within the 2 ventricles (Figure 7), the portion of myocyte aggregates running circumferentially was higher in the complex CHD heart compared with the control; while the mRV in the control heart had $\approx 2\%$ less circumferential myocardial strands compared with the mLV the percentage in the complex CHD heart in mRV and mLV are approximately equal (right ventricle= 14.7 ± 0.8 versus left ventricle= $14.0\pm 0.9\%$).

DISCUSSION

For the first time, we have nondestructively imaged and quantified the integrated myocardial macrostructure and microstructure of a whole *ex vivo* human fetal heart with complex CHD. We quantitatively extracted details of 3D microanatomy, namely cardiac myocyte organization, coronary circulation, and conduction system, and additionally showed how this can be used to (computationally) study the effect of the observed remodeling on electrical activation, as compared with a normal fetal heart.

Our approach shows a proof of principle for X-PCI, and subsequent analysis, to provide a novel promising way for capturing relevant detail of 3D myocyte arrangement and correlating with the conduction system and coronary supply without the need for sample processing, sectioning, and image registration. Similar results have been reported in a normal adult heart by means of micro-CT imaging⁸ but at $\approx 10\times$ lower resolution and requiring iodination of the sample to increase image contrast.

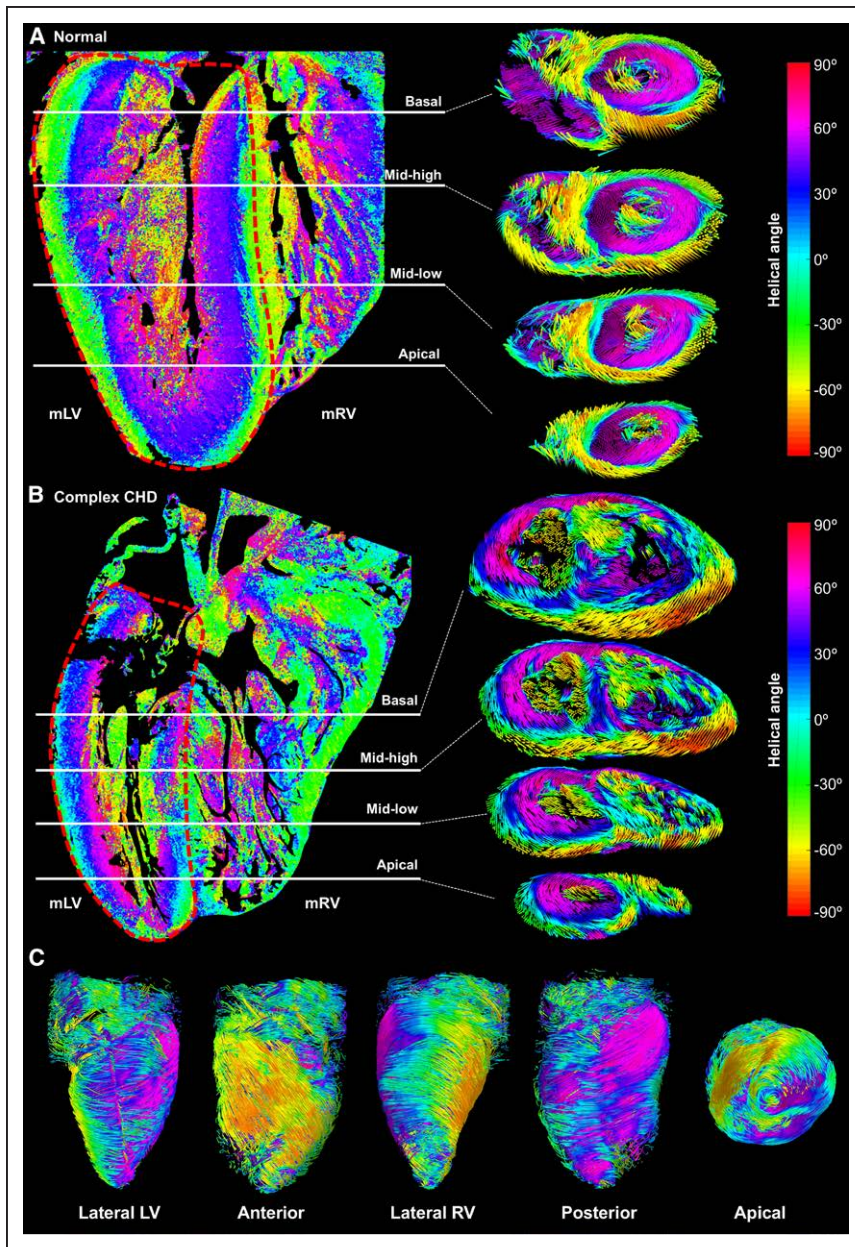


Figure 4. Quantification of helical angle (HA) in fetal hearts.

Longitudinal slice of the local HA of myocyte aggregates together with representation of the 3-dimensional HA vectors in 4 short-axis slices of both (A) normal and (B) complex congenital heart disease (CHD) fetal hearts at different apical-basal positions. C, From left to right: lateral left ventricle (LV), anterior, lateral right ventricle (RV), posterior, and apical views of the fetal heart with tracking based on v_3 eigenvector. Tracks were color coded by z-component value of the unit v_3 vector. mLV indicates morphologically left ventricle; and mRV, morphologically right ventricle.

The high-resolution images obtained by X-PCI allow us to discriminate the local predominant direction of myocyte aggregates using a 3D structure tensor approach and, in this initial study, to quantify the transmural distribution of HA. In both complex CHD and control, we observed well-conserved transmural variations in HA from endocardium to epicardium in the free wall of the mLV, similar to those reported in human adults or animals.^{10,12,25} The wider range of angle values and more regional differences in the HA of myocyte aggregates in comparison with previous studies is likely because of the immature fetal myocardium and higher resolution of our data, allowing us to quantify subtler local changes, as well as the ability to image the trabeculations in more detail. Our results support the hypothesis that cardiomyocytes are aggregated end to end forming a 3D mesh.

Our findings show that, even in the midtrimester, there is a smooth change in the HA across the thickness of the mLV rather than the abrupt change in HA that would be expected if the ventricles exist as a unique myocardial band.²⁶ Some authors have also described the existence of myocardial sheets or sheetlets. Although myocytes undoubtedly clump into linked colonies or bunches, we did not find evidence to support myocardial sheets in our fetal hearts, albeit that the supporting collagen network is known to be immature at this gestation.²⁷

In our case with complex CHD and mirror image arrangement of the ventricles, our results suggest that there is overall preservation of the change in HA of myocytic aggregates from endocardium to epicardium with a circumferential layer within mLV. The mRV is much more disorganized with an extensive deep trabecular layer

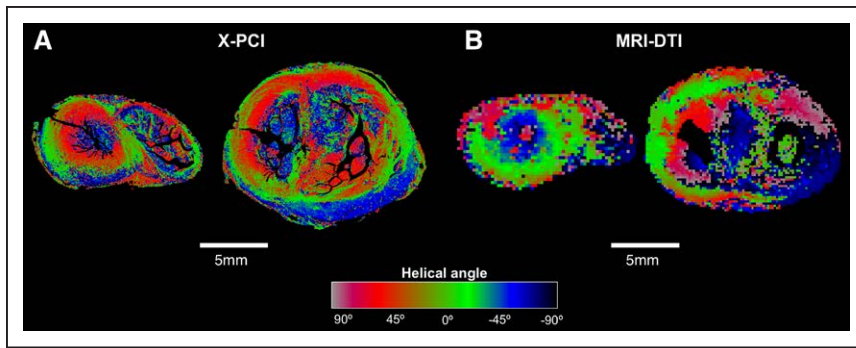


Figure 5. Comparison between X-ray phase-contrast imaging (X-PCI) and diffusion tensor magnetic resonance imaging (DT-MRI) helical angle (HA) analysis.

Estimation of HA in 2 different apical-basal image slices with (A) X-PCI and (B) DT-MRI analysis. All images were color coded by HA value.

and smaller circumferential layer. Moreover, although the transmural change in HA of myocyte aggregates in the mLV lateral wall, from endocardium to epicardium is linear and uniform between all short-axis slices, the septal transmural HA distribution is less linear and more heterogeneous across slices, particularly near the base of the heart. As has been reported in cases of situs inversus totalis,²⁴ we have observed that the orientation pattern of the myocyte aggregates changes from apex to the base, where the superficial (more epicardial) layer of myocyte aggregates in the complex CHD is thinner in the base compared with the apex.

These findings are clinically relevant because in the abnormal heart, the mLV was noted to be small on prenatal ultrasound. The parents had been counseled of the likelihood of a functionally univentricular palliation being required after birth (the Fontan circulation). In this setting, the mRV would have been the systemic ventri-

cle after corrective surgery. Although we cannot predict how the mRV would have developed through subsequent gestation and postnatally, it is well known that patients with right isomerism are particularly difficult to manage after birth and surgery, partly attributed to the constellation of lesions that are present.²⁸ It is possible that there would have been delayed recovery with normal remodeling of the mRV myocardium later in gestation. However, it is also possible that the regional wall disorganization documented in this heart could persist and that this would lead to abnormal regional function and wall stresses, contributing to abnormal global function, as well as development of remodeling and fibrosis, thus further contributing to morbidity or mortality.

Finally, our electrophysiological biophysical simulations show the potential of exploiting the high-resolution information retrieved from X-PCI images (detailed geometry integrated with local myocyte orientation) to

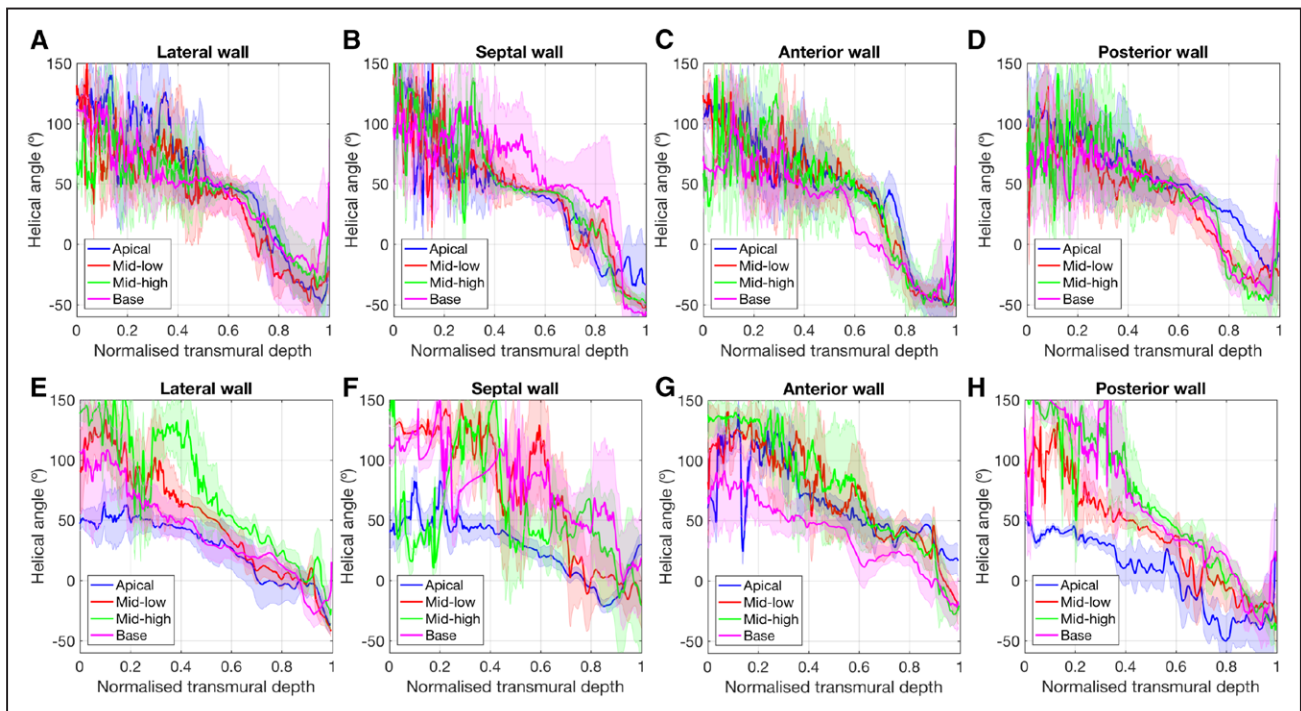


Figure 6. Transmural variation in helical angle.

Left ventricular transmural profiles of helical angles across 4 segments (lateral, septal, anterior, and posterior) in 4 different slices (apical, mid-low, mid-high, and basal) in the (A–D) normal and (E–H) complex congenital heart disease fetal heart.

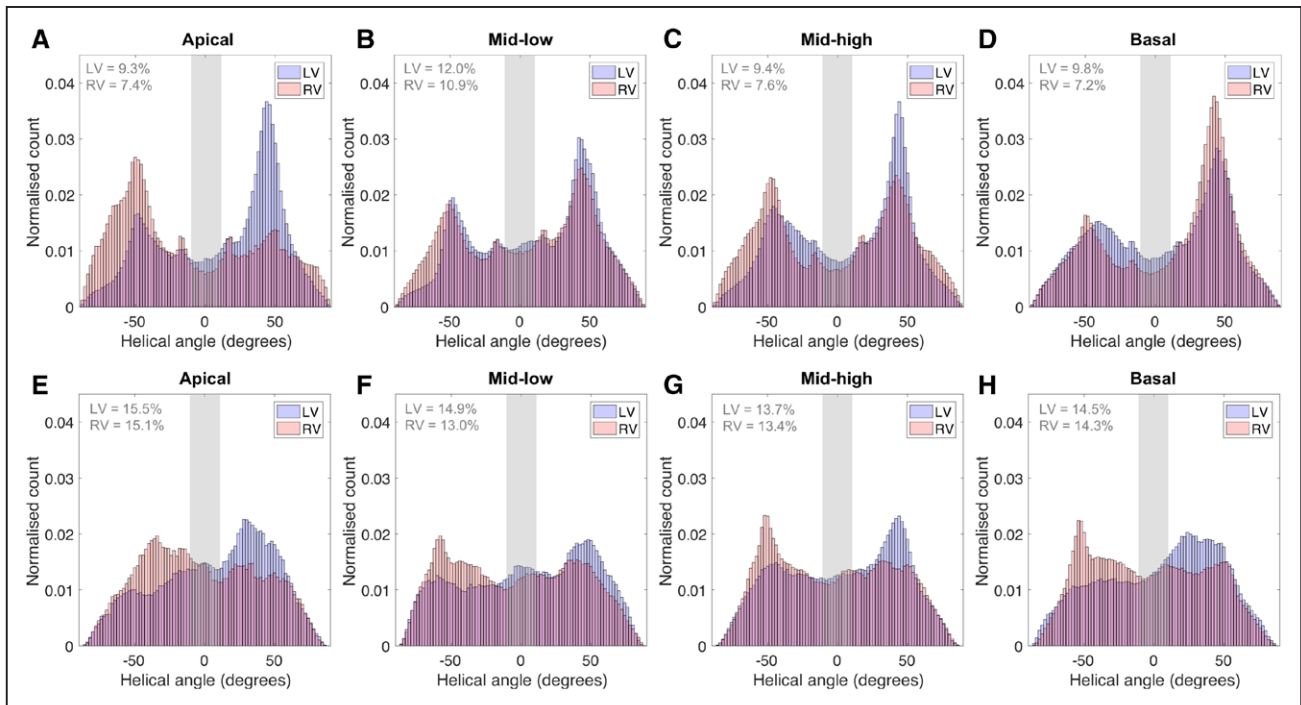


Figure 7. Histograms of helical angle in left ventricle (LV) and right ventricle (RV) of fetal hearts.

Histograms of helical angle for the LV and RV in 4 slices (apical, mid-low, mid-high, and basal) in the (A–D) normal and (E–H) complex congenital heart disease fetal hearts.

study cardiac electrical activity. Similar electrical activation studies have been demonstrated in a normal adult heart by Stephenson et al.⁸ Our initial results suggest the presence of electrical dyssynchrony in complex CHD compared with control, likely to lead to further mechanical inefficiency as often observed in CHD. Further delineation of activation after the specific path of the ventricular conduction system could be integrated to perform even more accurate and detail simulations, but this was out of the scope of this study.

Our study is proof of principle, but given the potential value of investigating developmental changes in the myocardium and microarchitecture in CHD, it strongly suggests that a comprehensive survey of fetal hearts with a wide spectrum of disease is warranted. Limitations might be availability of fetal material and access to time on synchrotrons worldwide, but with coordination of studies across centers, both of these factors could be overcome. With the rapid progress in synchrotron research and further clinical translation, it may, in the future, prove possible to perform noninvasive postmortem imaging of whole fetuses at higher resolutions than other modalities^{29,30} and even in vivo experiments. Translation of X-PCI to clinical scanners has already begun in the field of mammography for breast cancer detection,³¹ working toward in vivo assessment of tissue structure, fibrosis, and vessels without the use of contrast agents.

In conclusion, we have shown the potential of synchrotron X-PCI, to demonstrate macroanatomy and microanatomy of human fetal hearts in 3D, preserving invaluable

research material for further study and allowing detailed cocharacterization of the myocardium, coronaries, and conduction system thus providing novel, clinically relevant insight into the structure of fetal hearts with CHD.

ARTICLE INFORMATION

Received March 12, 2018; accepted June 21, 2018.

The Data Supplement is available at <https://www.ahajournals.org/doi/suppl/10.1161/CIRCIMAGING.118.007753>.

Correspondence

Patricia Garcia-Canadilla, PhD, Institute of Cardiovascular Science, University College London Institute of Child Health, 1st Floor Welcome Trust Bldg, 30 Guilford St, London United Kingdom. Email p.canadilla@ucl.ac.uk

Affiliations

Institute of Cardiovascular Science (P.G.-C., A.C.C.) and Division of Medicine, Centre for Advanced Biomedical Imaging (L.H.J., D.J.S.), University College London, United Kingdom. Department of Information and Communications Technologies, Universitat Pompeu Fabra, Barcelona, Spain (P.G.-C., C.Z., C.B., B.B.). Swiss Light Source, Paul Scherrer Institut, Villigen, Switzerland (H.D., A.B., M.S.). Institute for Biomedical Engineering, ETH Zurich, Zurich, Switzerland (H.D., M.S.). Faculty of Electrical Engineering and Computing, University of Zagreb, Zagreb, Croatia (V.B., S.L.). Barcelona Supercomputing Center-Centro Nacional de Supercomputación, Campus Nord Universitat Politècnica de Catalunya, Barcelona, Spain (J.A.-S., M.V.). IIIA-CSIC, Bellaterra, Spain (M.V.). Diamond Manchester Imaging Branchline (I13-2), Diamond Lightsource, Oxford, United Kingdom (C.R.). Institución Catalana de Investigación y Estudios Avanzados, Barcelona, Spain (B.B.).

Acknowledgments

We acknowledge the Paul Scherrer Institute, Villigen, Switzerland, and Diamond Light Source, Oxford (United Kingdom), for provision of synchrotron radiation beamtime at beamline X02DA TOMCAT and at beamline I13-2, respectively. Dr Garcia-Canadilla acknowledges EMBO for a short-term fellowship

at the Paul Scherrer Institute, Villigen, Switzerland, and Fundació Daniel Bravo Andreu for a research fellowship at University College London, London.

Sources of Funding

This study was partially supported by the Spanish Ministry of Economy and Competitiveness (grant TIN2014-52923-R and the Maria de Maeztu Units of Excellence Programme, MDM-2015-0502) and FEDER. Dr Butakoff is supported by Fundació La Marató de TV3 (Spain), grant No. 20154031. Dr Aguado-Sierra is supported by the Center of Excellence CompBioMed funded under H2020-EU.1.4.1.3. under grant agreement No. 675451. Dr Stuckey is supported by the British Heart Foundation under grant No. FS/15/33/31608.

Disclosures

None.

REFERENCES

- Dolk H, Loane M, Garne E; European Surveillance of Congenital Anomalies (EUROCAT) Working Group. Congenital heart defects in Europe: prevalence and perinatal mortality, 2000 to 2005. *Circulation*. 2011;123:841–849. doi: 10.1161/CIRCULATIONAHA.110.958405
- Anderson RH, Smerup M, Sanchez-Quintana D, Loukas M, Lunkenheimer PP. The three-dimensional arrangement of the myocytes in the ventricular walls. *Clin Anat*. 2009;22:64–76. doi: 10.1002/ca.20645
- Torrent-Guasp F, Ballester M, Buckberg GD, Carreras F, Flotas A, Carrió I, Ferreira A, Samuels LE, Narula J. Spatial orientation of the ventricular muscle band: physiologic contribution and surgical implications. *J Thorac Cardiovasc Surg*. 2001;122:389–392. doi: 10.1067/mtc.2001.113745
- Henderson DJ, Anderson RH. The development and structure of the ventricles in the human heart. *Pediatr Cardiol*. 2009;30:588–596. doi: 10.1007/s00246-009-9390-9
- Matsui H, Mohun T, Gardiner HM. Three-dimensional reconstruction imaging of the human foetal heart in the first trimester. *Eur Heart J*. 2010;31:415. doi: 10.1093/eurheartj/ehp511
- Mekkaoui C, Porayette P, Jackowski MP, Kostis WJ, Dai G, Sanders S, Sosnovik DE. Diffusion MRI tractography of the developing human fetal heart. *PLoS One*. 2013;8:e72795. doi: 10.1371/journal.pone.0072795
- Stephenson RS, Boyett MR, Hart G, Nikolaidou T, Cai X, Corno AF, Alphonso N, Jeffery N, Jarvis JC. Contrast enhanced micro-computed tomography resolves the 3-dimensional morphology of the cardiac conduction system in mammalian hearts. *PLoS One*. 2012;7:e35299. doi: 10.1371/journal.pone.0035299
- Stephenson RS, Atkinson A, Kottas P, Perde F, Jafarzadeh F, Bateman M, Iaizzo PA, Zhao J, Zhang H, Anderson RH, Jarvis JC, Dobrzynski H. High resolution 3-Dimensional imaging of the human cardiac conduction system from microanatomy to mathematical modeling. *Sci Rep*. 2017;7:7188. doi: 10.1038/s41598-017-07694-8
- Mirea I, Varray F, Zhu YM, Fanton L, Langer M, Jouk PS, Michalowicz G, Usson Y, Magnin IE. Very high-resolution imaging of post-mortem human cardiac tissue using X-ray phase contrast tomography. In: *Functional Imaging and Modeling of the Heart*. Maastricht, The Netherlands: Springer International Publishing; 2015:172–179.
- Gonzalez-Tendero A, Zhang C, Balicevic V, Cárdenes R, Loncaric S, Butakoff C, Paun B, Bonnin A, Garcia-Cañadilla P, Muñoz-Moreno E, Gratacós E, Crispí F, Bijnens B. Whole heart detailed and quantitative anatomy, myofiber structure and vasculature from X-ray phase-contrast synchrotron radiation-based micro computed tomography. *Eur Heart J Cardiovasc Imaging*. 2017;18:732–741. doi: 10.1093/ehjci/jew314
- Kaneko Y, Shinohara G, Hoshino M, Morishita H, Morita K, Oshima Y, Takahashi M, Yagi N, Okita Y, Tsukube T. Intact imaging of human heart structure using X-ray phase-contrast tomography. *Pediatr Cardiol*. 2017;38:390–393. doi: 10.1007/s00246-016-1527-z
- Balićević V, Lončarić S, Cárdenes R, Gonzalez-Tendero A, Paun B, Crispí F, Butakoff C, Bijnens B. Assessment of Myofiber Orientation in High Resolution Phase-Contrast CT Images. In: *Functional Imaging and Modeling of the Heart*. Maastricht, The Netherlands: Springer International Publishing; 2015:111–119.
- Cook AC. Cardiac Morphology. 2018. <http://www.cardiacmorphology.com/>. Accessed October 2, 2018.
- Paganin D, Mayo SC, Gureyev TE, Miller PR, Wilkins SW. Simultaneous phase and amplitude extraction from a single defocused image of a homogeneous object. *J Microsc*. 2002;206(pt 1):33–40.
- Marone F, Stampanoni M. Regriding reconstruction algorithm for real-time tomographic imaging. *J Synchrotron Radiat*. 2012;19(pt 6):1029–1037. doi: 10.1107/S0909049512032864
- Sommer C, Strähle C, Köthe U, Hamprecht FA. Ilastik: interactive learning and segmentation toolkit. In: *Proceedings - International Symposium on Biomedical Imaging. IEEE*; 2011:230–233.
- Cibc. Seg3D: Volumetric Image Segmentation and Visualization. Scientific Computing and Imaging Institute (SCI). 2013. <http://www.seg3d.org>. Accessed October 2, 2018.
- Fedorov A, Beichel R, Kalpathy-Cramer J, Finet J, Fillion-Robin JC, Pujol S, Bauer C, Jennings D, Fennessy F, Sonka M, Buatti J, Aylward S, Miller JV, Pieper S, Kikinis R. 3D Slicer as an image computing platform for the Quantitative Imaging Network. *Magn Reson Imaging*. 2012;30:1323–1341. doi: 10.1016/j.mri.2012.05.001
- Shinohara G, Morita K, Hoshino M, Ko Y, Tsukube T, Kaneko Y, Morishita H, Oshima Y, Matsuhisa H, Iwaki R, Takahashi M, Matsuyama T, Hashimoto K, Yagi N. Three dimensional visualization of human cardiac conduction tissue in whole heart specimens by high-resolution phase-contrast CT imaging using synchrotron radiation. *World J Pediatr Congenit Heart Surg*. 2016;7:700–705. doi: 10.1177/2150135116675844
- Cook PA, Bai Y, Nedjati-Gilani S, Seunarine KK, Hall MG, Parker GJ, Alexander DC. Camino: open-source diffusion-MRI reconstruction and processing. In: 14th Scientific Meeting of the International Society for Magnetic Resonance in Medicine. 2006:2759.
- Smith A, Ho SY, Anderson RH, Connell MG, Arnold R, Wilkinson JL, Cook AC. The diverse cardiac morphology seen in hearts with isomerism of the atrial appendages with reference to the disposition of the specialised conduction system. *Cardiol Young*. 2006;16:437–454. doi: 10.1017/S1047951106000382
- Ho SY, Fagg N, Anderson RH, Cook A, Allan L. Disposition of the atrio-ventricular conduction tissues in the heart with isomerism of the atrial appendages: its relation to congenital complete heart block. *J Am Coll Cardiol*. 1992;20:904–910.
- Anderson RH, Ho SY, Redmann K, Sanchez-Quintana D, Lunkenheimer PP. The anatomical arrangement of the myocardial cells making up the ventricular mass. *Eur J Cardiothorac Surg*. 2005;28:517–525. doi: 10.1016/j.ejcts.2005.06.043
- Delhaas T, Kroon W, Decaluwe W, Rubbens M, Bovendeerd P, Arts T. Structure and torsion of the normal and situs inversus totalis cardiac left ventricle. I. Experimental data in humans. *Am J Physiol Heart Circ Physiol*. 2008;295:H197–H201. doi: 10.1152/ajpheart.00876.2007
- Teh I, Burton RA, McClymont D, Capel RA, Aston D, Kohl P, Schneider JE. Mapping cardiac microstructure of rabbit heart in different mechanical states by high resolution diffusion tensor imaging: a proof-of-principle study. *Prog Biophys Mol Biol*. 2016;121:85–96. doi: 10.1016/j.pbiomolbio.2016.06.001
- Maclver DH, Stephenson RS, Jensen B, Agger P, Sánchez-Quintana D, Jarvis JC, Partridge JB, Anderson RH. The end of the unique myocardial band: Part I. Anatomical considerations. *Eur J Cardiothorac Surg*. 2018;53:112–119. doi: 10.1093/ejcts/ezx290
- Jackson M, Connell MG, Smith A. Development of the collagen network of the human fetal myocardium: an immunohistochemical study. *Int J Cardiol*. 1993;41:77–86.
- Graupner O, Enzensberger C, Wieg L, Willruth A, Steinhard J, Gembruch U, Doelle A, Bahlmann F, Kawecky A, Degenhardt J, Wolter A, Herrmann J, Axt-Fliedner R; Fetal Cardiac Imaging Research Group Germany. Evaluation of right ventricular function in fetal hypoplastic left heart syndrome by color tissue Doppler imaging. *Ultrasound Obstet Gynecol*. 2016;47:732–738. doi: 10.1002/uog.14940
- Arthurs OJ, Thayyil S, Olsen OE, Addison S, Wade A, Jones R, Norman W, Scott RJ, Robertson NJ, Taylor AM, Chitty LS, Sebire NJ, Owens CM; Magnetic Resonance Imaging Autopsy Study (MaRIAS) Collaborative Group. Diagnostic accuracy of post-mortem MRI for thoracic abnormalities in fetuses and children. *Eur Radiol*. 2014;24:2876–2884. doi: 10.1007/s00330-014-3313-8
- Lombardi CM, Zambelli V, Botta G, Moltrasio F, Cattoretti G, Lucchini V, Fesslova V, Cuttin MS. Postmortem microcomputed tomography (micro-CT) of small fetuses and hearts. *Ultrasound Obstet Gynecol*. 2014;44:600–609. doi: 10.1002/uog.13330
- Castelli E, Tonutti M, Arfelli F, Longo R, Quaia E, Rigon L, Sanabor D, Zanconati F, Dreossi D, Abrami A, Quai E, Bregant P, Casarin K, Chenda V, Menk RH, Rokvic T, Vascotto A, Tromba G, Cova MA. Mammography with synchrotron radiation: first clinical experience with phase-detection technique. *Radiology*. 2011;259:684–694. doi: 10.1148/radiol.11100745